

Time-dependent prestress loss behavior of girders in Missouri bridge A7957 compared with a U.S. data set of high-performance concrete bridge girders

Hayder H. Alghazali and John J. Myers

Long service lives and low maintenance costs for bridges are attainable with sustainable and durable advanced concrete materials. Constructing a bridge with these new types of concrete often requires monitoring to evaluate its performance and various aspects of its structural behavior. A comprehensive structure health monitoring system, including sensors that measure parameters related to performance and structural behavior, can be the most efficient way to obtain actionable data on bridge performance. In this study, high-strength concrete (HSC) and self-consolidating concrete (SCC) with two different performance levels were used in the construction of the superstructure of a bridge.

- In this study, six precast, prestressed concrete girders were constructed and instrumented to measure prestress losses of bridge A7957 in Missouri.
- High-strength concrete, high-strength self-consolidating concrete, and normal-strength self-consolidating concrete were used to construct the bridge girders.
- The measured short- and long-term prestress losses were compared with those obtained using different empirical models and present a comparison of measured prestress losses with data reported in the literature for different concrete types.

HSC gives bridge designers greater flexibility for the design of precast, prestressed concrete structures. It permits longer-span structures that result from more compact sections. Using HSC can lower the initial project cost by allowing longer spans for a given girder cross section or by increasing the girder spacing and reducing the number of girders.¹ ACI 363R-10² defines HSC as a type of concrete with a 28-day compressive strength of 8000 psi (55 MPa) or greater. The high strength is made possible by reducing porosity, inhomogeneity, and microcracks in the hydrated cement paste and the transition zone. HSC is considered to be more durable than conventional concrete. However, its production requires more attention to quality control than conventional concrete. Mixture proportions

for HSC require the use of strong, durable aggregate and often a high cementitious material content, which generally results in a lower water–cementitious materials ratio. Mixture proportions for an HSC can vary depending on locally available materials that allow the fresh concrete to be workable and ensure that the strength development is as specified by the designer. With the variety of constituent materials and requirements, many performance-related issues require closer attention. Differences in the amount of time-dependent losses are one example of an area currently under investigation. Understanding and predicting prestress losses are essential in the design of a prestressed concrete beam. If care is not taken to determine the prestress losses at various stages, the design can result in a poor serviceability state of behavior.

SCC was developed in Japan in the 1980s and started to be used widely in the United States in the 1990s. It can be consolidated into every corner of formwork by means of its own weight and without the need for mechanical consolidation.³ High-strength SCC is a recent innovation developed by civil engineers. It has all of the benefits of self-consolidating concrete (such as flowability and stability) with the added benefit of increased strength. It is beneficial in cases that require a congested steel cross section because it can envelop and encapsulate the steel reinforcement, even in congested steel areas.⁴ High-strength SCC is a type of material for which the material proportions can be modified (for example, reducing the content and size of the coarse aggregate or increasing the paste volume to enhance fluidity) compared with either HSC or SCC. A question is raised here regarding SCC's constituent make-up and effect of fluidity on the structural behavior of high-strength SCC. Differences in the engineering properties (such as time-dependent losses and the modulus of elasticity in concrete structure applications) are examples of an area under investigation. The efficient design of a prestressed concrete member needs to be well understood.

Prestress losses are the losses in tensile stress of prestressing steel that affect the performance of a prestressed concrete section. The tensile force in the tendon does not stay constant according to the recorded value in the jacking gauge but changes over time. The losses are classified into two categories: immediate and long-term (or time-dependent) losses. Immediate losses take place during prestressing of the tendon and transfer the prestress to the concrete member. The elastic shortening and slip of the anchorage are immediate losses. Losses due to creep of the concrete, shrinkage of the concrete, and relaxation of the tendon are considered time-dependent losses.⁵ There are numerous prestress loss estimation procedures that can be found in a variety of sources. The most commonly used approaches to determine the components of prestress losses are provided by the American Association of State Highway and Transportation Officials' *AASHTO LRFD Bridge Design*

*Specifications*⁶ and the *PCI Design Handbook: Precast and Prestressed Concrete*.⁷

A limited number of full-scale studies have been conducted to determine the long-term behavior of prestressed HSC and high-strength SCC beams. In a recent study by Myers et al.,¹ two precast, prestressed HSC and high-strength SCC bridges were instrumented. The HSC bridge spans a length of 48 ft (15 m) and has a width of 10 ft (3 m). The high-strength SCC bridge spans a length of 34 ft (10 m) and has a width of 10 ft. A total of 32 vibrating wire strain gauges with built-in thermistors were used in the beams and decks. Two data acquisition system boxes were used to monitor both bridges. The researchers incorporated two commonly used loss estimate models for calculating total prestress losses, from the AASHTO LRFD specifications and the *PCI Design Handbook*. The researchers reported that the losses in the HSC and high-strength SCC bridges were approximately 6.21% and 4.86%, respectively, of the nominal jacking stress. It was concluded that the AASHTO LRFD specifications model overestimated the prestress loss of HSC by 23% and high-strength SCC by 57% when the measured modulus of elasticity of the material was used in the predicted model. The *PCI Design Handbook* model was not as accurate and overestimated the total prestress loss by 24% for HSC and 85% for high-strength SCC when the measured modulus of elasticity of the material was used in the predicted model.

In a study conducted by Roller et al.,⁸ four 131 ft (39.9 m) long full-scale bridge girders were instrumented to evaluate the prestress losses in HSC bulb-tee girders for the Rigolets Pass Bridge in Louisiana. The total measured prestress losses derived from concrete strains corrected for temperature and load effects were found to be lower than corresponding values calculated using the AASHTO LRFD specifications.

Brewe and Myers⁹ conducted a study on six reduced-scale high-strength SCC prestressed girders. They used a demountable mechanical strain gauge to monitor prestress losses. The measured prestress losses were compared with various code models. The authors concluded that the *PCI Design Handbook* method overestimated the prestress losses by approximately 21%, the refined method in the 2007 AASHTO LRFD specifications underestimated the losses by approximately 18%, and the 2004 AASHTO LRFD specifications overestimated the losses by approximately 10%. They also believed that the 2007 AASHTO LRFD specifications method would provide superior results for most projects because this method uses improved equations with fewer assumptions.

Bridge description

Bridge A7957 is located on Highway 50 in Osage County, Mo. The bridge has three spans with precast, prestressed

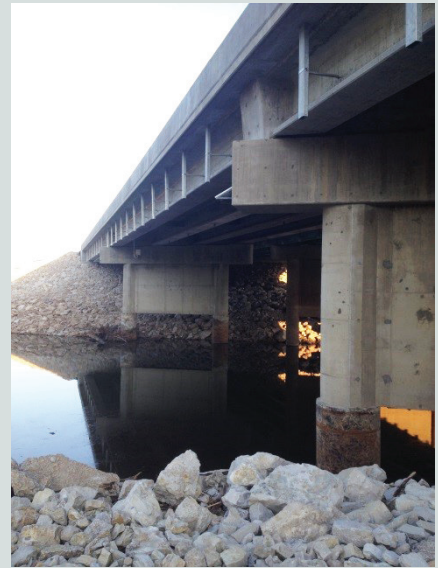


Figure 1. Side and front views of bridge A7957 located on Highway 50 near Linn, Mo.

concrete girders. The bridge was designed to be simply supported for dead load and continuous for live load via a cast-in-place concrete deck (**Fig. 1**). Each span was designed with concrete mixtures of varying compressive strengths. The two exterior spans are 100 ft (30 m) long, and one interior span is 120 ft (37 m) long. The superstructure is supported by two intermediate bents and two abutments. The bridge has a superelevation of 2.0%.

Each span implemented four precast, prestressed Nebraska University (NU) 53 girders. The girder's cross section provides several advantages during construction, giving designers more flexibility to increase strand capacity and reduce stress concentration in the edges by curved fillets

(**Fig. 2**). The first- and third-span beams were prestressed with 30 Grade 270 (1860 MPa) steel tendons: 20 were straight and 10 were harped at double points. The 0.6 in. (15 mm) diameter tendons were seven-wire, low-relaxation strands. Four additional $\frac{3}{8}$ in. (9.5 mm) diameter prestressing strands were added within the top flange of each girder for crack control. Span two girders were prestressed with the same type of strands; however, 28 strands were straight and 10 strands were harped at double points. D20 (MD 130) welded-wire reinforcement was provided for shear resistance at spacing intervals of 4, 8, and 12 in. (100, 200, and 300 mm) along the length of the girder. The jacking force per strand was 44 kip (196 kN), slightly overstressed to 45 kip (200 kN) to compensate

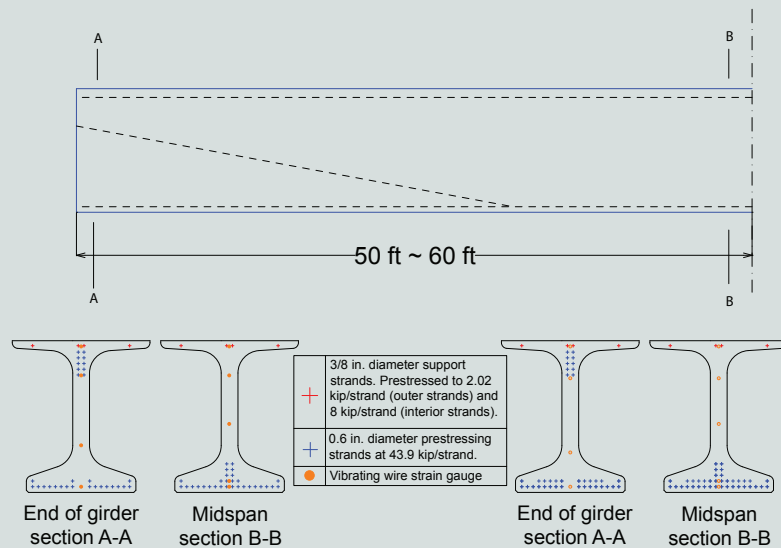


Figure 2. Cross-section view of Nebraska University 53 girder. Note: 1 in. = 25.4 mm; 1 ft = 0.305 m; 1 kip = 4.448 kN.

Table 1. Concrete mixture proportions

Material	Type	Quantity		
		HSC	HS-SCC	NS-SCC
Coarse aggregate, lb/yd ³	¾ in. crushed stone, grade E dolomite	1780	n/a	n/a
	½ in. crushed stone, grade E dolomite	n/a	1340	1476
Fine aggregate, lb/yd ³	River sand	1085	1433	1433
Cement, lb/yd ³	Portland cement, Type I	800	850	750
Water/cement	n/a	0.32	0.33	0.35
Chemical admixtures (oz/yd ³)	Air entraining agent	8	17	17
	Type D water-reducing admixture and set-retarding admixture	9.2	76.5	67.5
	Type F high-range water-reducing admixture	17.2	25.5	25.5

Note: HSC = high-strength concrete; HS-SCC = high-strength self-consolidating concrete; n/a = not applicable; NS-SCC = normal-strength self-consolidating concrete. 1 in. = 25.4 mm; 1 lb/yd³ = 0.593 kg/m³; 1 oz/yd³ = 37 g/m³.

Table 2. Summary of fresh properties, tests, and results

Rheological property	Test method	Member (span girder)					
		S1-G3	S1-G4	S2-G3	S2-G4	S3-G3	S3-G4
Air, %	ASTM C231	6.9	6.9	7.5	7.6	6	8.3
Slump or slump flow, in.	ASTM C1611	9	9	27	26	26.5	26.5
J-ring, in.	ASTM C1621	n/a	n/a	26.5	25	25.5	25.5
Local temperature, °F	n/a	n/a	n/a	78	76	74	78
Segregation column S, %	ASTM C1610	n/a	n/a	0	0.56	n/a	0
Concrete temperature, °F	ASTM C1064	73	73	n/a	80	80	82

Note: n/a = not applicable. 1 in. = 25.4 mm; °C = (°F - 32)/1.8.

Table 3. Summary of mechanical properties, tests, and results

Test	Test method	Specimens	Concrete age	Member (span girder)					
				S1-G3	S1-G4	S2-G3	S2-G4	S3-G3	S3-G4
Compressive strength, psi	ASTM C39	4 in. diameter × 8 in. long cylinder	Release	6896	7635	8516	8141	6924	6434
			28 days	10,774	9733	11,238	10,433	9966	9135
			365 days	10,236	10,642	11,121	11,551	9604	8642
Modulus of elasticity, ksi	ASTM C469		Release	4435	4717	5328	4697	4706	4212
			28 days	5223	5143	5710	5204	5256	4792
			365 days	5648	5604	5575	5800	5771	5452
Modulus of rupture, psi	ASTM C78	6 × 6 × 21/24 in. beams	28 days	587	653	691	633	817	640
Coefficient of thermal expansion, με/°F	ASTM C490	4 in. diameter × 24 in. long cylinder	180 days	4.97		5.51		6.28	

Note: 1 in. = 25.4 mm; 1 psi = 6.895 kPa; 1 ksi = 6.895 MPa; °C = (°F - 32)/1.8.

for anchorage losses. To produce a high early strength, a steam-curing regime was used to accelerate the hydration process of all of the precast, prestressed concrete girders. The maximum steam regime temperature did not exceed 120°F (49°C). The maximum temperatures were held for a period sufficient to develop the required strength (14 to 38 hours).

The target 28-day compressive strength of the HSC and normal-strength SCC was 8000 psi (55 MPa), and the specified release strength was 6500 psi (45 MPa). However, the high-strength SCC had a 10,000 psi (69 MPa) target 28-day compressive strength and a release compressive strength of 8000 psi. **Table 1** presents the mixture proportions of each type of concrete. The job-specific specifications for this project set a minimum required coarse aggregate content of 48% (of the total coarse and fine aggregate contents) for the SCC mixtures. This was done to avoid a low modulus of elasticity concrete that could result if a very low coarse aggregate content were used in the SCC mixtures. Lower modulus of elasticity concrete would have resulted in higher overall prestress losses. The precast concrete girders and deck panels were fabricated in August 2013 in Bonne Terre, Mo. Erection began in September 2013. The deck slab was cast from the east to the west sides of the girder, after erection of girders at the site in October 2013. The bridge entered service (opened to traffic) in mid-2014 after the roadway was completed.

Monitoring system

High-strength concrete, high-strength SCC, and normal-strength SCC girders were produced for spans 1, 2, and 3 of bridge A7957, respectively. They were instrumented to obtain data for the measured strain and temperature. Six instrumented girders (S1-G3, S1-G4, S2-G3, S2-G4, S3-G3, and S3-G4) were monitored from fabrication through service life.

Vibrating wire strain gauges

A total of 86 vibrating wire strain gauges with built-in thermistors were used to measure the strain and temperature of the precast, prestressed concrete girders. The standard pattern at the midspan consisted of five gauges over the height of the girder and two more in the slab above the girder. During construction, vibrating wire strain gauge readings were made before strand release, after strand release, during transportation and erection, and before and after casting the deck slab concrete. Monitoring of the bridge is ongoing.

Data acquisition system

The data from the vibrating wire strain gauges were recorded by two wireless data acquisition system boxes.

Following the erection of the girders, the data acquisition system was anchored to the interior side of the intermediate bent pier caps for long-term monitoring. A cellular antenna, which was also anchored to the interior side of the bent 2 pier cap, was used to send the data from the data acquisition system in real time back to the researchers during fabrication of the precast, prestressed concrete girders and at the various stages of the bridge construction. Measurements were taken at five-minute intervals.

Material properties

Material property tests were performed on specimens collected from the same batch of concrete as the girders to have adequate predictions for the prestress losses. All the tests follow standard ASTM guidelines.¹⁰⁻¹⁸ **Tables 2 and 3** present a summary of the tests, test methods, and results.

Prestress losses

Elastic shortening losses

Elastic shortening is the loss of prestress force that takes place when a strand becomes shorter. The forms are stripped, and the prestressing strands are released after adequate strength is added to the casting bed. As a result, the concrete and strands shorten under the load. Elastic shortening loss represents a significant portion of the total prestress loss. The vibrating wire strain gauges embedded in the concrete girder were used to measure elastic shortening indirectly. These measurements were obtained by subtracting the strain reading immediately after release from the baseline strain measurement recorded just before release. Measurements were taken at the level of the strand's center of gravity of the steel. The measuring strain was corrected for thermal effect and multiplied by the modulus of elasticity of the prestressing strands E_{ps} (28,500 ksi [197 MPa]) to determine measured elastic shortening prestress losses (Eq. [1]). Equation (2) was used to calculate the change in stress from elastic shortening $\Delta f_{ES, Calculated}$.

$$\Delta f_{ES, Measured} = E_{ps} \epsilon_{cgs} \quad (1)$$

where

$\Delta f_{ES, Measured}$ = measured change in stress from elastic shortening

ϵ_{cgs} = strain at the centroid of the prestressing steel

$$\Delta f_{ES, Calculated} = \frac{E_{ps}}{E_{ci}} f_{cgs} \quad (2)$$

where

$$E_c = 40,000\sqrt{f'_c} + 10^6 \quad (5)$$

E_{ci} = modulus of elasticity of the concrete at release

f_{cgs} = stress of the concrete at the centroid of the prestressing strands

Equation (3) was used to estimate f_{cgs} .

$$f_{cgs} = \frac{P}{A} + \frac{Pe^2}{I_g} - \frac{Me}{I_g} \quad (3)$$

where

P = estimated force immediately after release

A = gross cross-sectional area

e = eccentricity of the strand

I_g = gross moment of inertia (uncracked section)

M = moment applied to the beam

The measured elastic shortening losses were determined and compared with the empirical equations adopted by the 2012 AASHTO LRFD specifications and the 2007 *PCI Design Handbook* with the actual and approximate moduli of elasticity. The modulus of elasticity plays an important role in predicting elastic shortening losses. Coarse aggregate typically makes up the majority of a concrete mixture; therefore, the behavior of the final hardened concrete depends on the type and quantity of coarse aggregate. From this point, the expression specified in the American Concrete Institute's (ACI's) *Building Code Requirements for Structural Concrete (ACI 318-14)* and *Commentary (ACI 318R-14)*¹⁹ was selected (Eq. [4])² to predict the modulus of elasticity. In addition, the expression adopted by ACI 363R-10² was also used to determine the modulus of elasticity (Eq. [5]). **Tables 4** through **6** display the results of measured and predicted elastic shortening using the actual and approximate modulus of elasticity.

$$E_c = 33w_c^{1.5}\sqrt{f'_c} \quad (4)$$

where

E_c = concrete modulus of elasticity

w_c = concrete density

f'_c = concrete compressive strength

The measured elastic shortening values were typically higher than those predicted by the AASHTO LRFD specifications and the *PCI Design Handbook*. The method given in the AASHTO LRFD specifications underestimated the elastic shortening losses by 25%. However, the *PCI Design Handbook* method tended to underestimate the elastic shortening losses of HSC by 35%. As a result, the AASHTO LRFD specifications method was considered more accurate than the *PCI Design Handbook* method.

Comparison for total prestress losses

The total prestress losses in precast, prestressed concrete girders consist of elastic shortening loss, shrinkage of concrete, creep of concrete, and relaxation of strand, which are considered for serviceability cases.^{20,21} Relaxation losses were obtained for the tendons stressed beyond 55% based on the measured prestressing force using the relaxation model (Eq. [6]).²² These losses do not affect the ultimate strength of a girder, but they may lead to poor prediction of service camber and deflection.²³ Empirical models have been provided by the AASHTO LRFD specifications and *PCI Design Handbook* to determine the components of prestress losses separately.

$$\Delta f_{RE} = f'_{pi} \frac{\log_{10} t}{45} \left(\frac{f'_{pi}}{f_{py}} - 0.55 \right) \quad (6)$$

where

f'_{pi} = initial stress of prestressing tendons

t = time after prestressing

f_{py} = specified yield strength of prestressing tendons

The strain readings at the center of gravity of the steel from the vibrating wire strain gauges were used to measure the total prestress loss in the concrete girder. These values were determined through strain compatibility using the portion of prestress loss due to elastic shortening, creep, and shrinkage. The relaxation losses were estimated analytically. The measured prestress losses were compared with predicted losses calculated according to the AASHTO LRFD specifications and the *PCI Design Handbook* using the measured elastic modulus of concrete.

The total measured losses of the HSC girders averaged 38.6 ksi (266 MPa), or 19.4% of the nominal jacking stress of 199 ksi (1370 MPa). However, the total measured losses

Table 4. Elastic shortening losses of high-strength concrete

Result method	S1-G3				S1-G4			
	Microstrain	Stress, psi	Jacking, [‡] %	<i>m/p</i> ratio	Microstrain	Stress, psi	Jacking, [‡] %	<i>m/p</i> ratio
Measured	632 × 10 ⁻⁶	18,024	9.1	1.00	710 × 10 ⁻⁶	20,235	10.2	1.00
AASHTO*	521 × 10 ⁻⁶	14,855	7.5	1.21	490 × 10 ⁻⁶	13,968	7.0	1.45
AASHTO [†]	483 × 10 ⁻⁶	13,769	6.9	1.31	459 × 10 ⁻⁶	13,086	6.6	1.55
PCI*	452 × 10 ⁻⁶	12,869	6.5	1.40	425 × 10 ⁻⁶	12,100	6.1	1.67
PCI [†]	476 × 10 ⁻⁶	13,580	6.8	1.33	461 × 10 ⁻⁶	13,127	6.6	1.54

Note: AASHTO = AASHTO LRFD Bridge Design Specifications; *m* = measured loss; *n/a* = not applicable; *n.d.* = no data; *p* = predicted loss; PCI = PCI Design Handbook: Precast and Prestressed Concrete. 1 psi = 6.895 kPa.

* Methods using measured modulus of elasticity.

[†] Methods using approximate modulus of elasticity (Eq. [4] for AASHTO and Eq. [5] for PCI).

[‡] Percentage of total prestress loss stress to nominal jacking stress.

Table 5. Elastic shortening losses of high-strength self-consolidating concrete

Result method	S2-G3				S2-G4			
	Microstrain	Stress, psi	Jacking, [‡] %	<i>m/p</i> ratio	Microstrain	Stress, psi	Jacking, [‡] %	<i>m/p</i> ratio
Measured	n.d.	n/a	n/a	n/a	732 × 10 ⁻⁶	20,866	10.5	1.00
AASHTO*	524 × 10 ⁻⁶	14,940	7.5	n/a	524 × 10 ⁻⁶	14,940	7.5	1.40
AASHTO [†]	525 × 10 ⁻⁶	14,971	7.5	n/a	537 × 10 ⁻⁶	15,312	7.7	1.36
PCI*	452 × 10 ⁻⁶	12,876	6.5	n/a	511 × 10 ⁻⁶	14,572	7.3	1.43
PCI [†]	533 × 10 ⁻⁶	15,179	7.6	n/a	541 × 10 ⁻⁶	15,409	7.7	1.35

Note: AASHTO = AASHTO LRFD Bridge Design Specifications; *m* = measured loss; *n/a* = not applicable; *n.d.* = no data; *p* = predicted loss; PCI = PCI Design Handbook: Precast and Prestressed Concrete. 1 psi = 6.895 kPa.

* Methods using measured modulus of elasticity.

[†] Methods using approximate modulus of elasticity (Eq. [4] for AASHTO and Eq. [5] for PCI).

[‡] Percentage of total prestress loss stress to nominal jacking stress.

Table 6. Elastic shortening losses of normal-strength self-consolidating concrete

Result method	S3-G3				S3-G4			
	Microstrain	Stress, psi	Jacking, [‡] %	<i>m/p</i> ratio	Microstrain	Stress, psi	Jacking, [‡] %	<i>m/p</i> ratio
Measured	605 × 10 ⁻⁶	17,240	8.7	1.00	618 × 10 ⁻⁶	17,621	8.9	1.00
AASHTO*	491 × 10 ⁻⁶	13,998	7.0	1.23	491 × 10 ⁻⁶	13,998	7.0	1.26
AASHTO [†]	482 × 10 ⁻⁶	13,741	6.9	1.25	500 × 10 ⁻⁶	14,255	7.2	1.24
PCI*	425 × 10 ⁻⁶	12,126	6.1	1.42	500 × 10 ⁻⁶	14,255	7.2	1.24
PCI [†]	476 × 10 ⁻⁶	13,561	6.8	1.27	488 × 10 ⁻⁶	13,897	7.0	1.27

Note: AASHTO = AASHTO LRFD Bridge Design Specifications; *m* = measured loss; *n/a* = not applicable; *n.d.* = no data; *p* = predicted loss; PCI = PCI Design Handbook: Precast and Prestressed Concrete. 1 psi = 6.895 kPa.

* Methods using measured modulus of elasticity.

[†] Methods using approximate modulus of elasticity (Eq. [4] for AASHTO and Eq. [5] for PCI).

[‡] Percentage of total prestress loss stress to nominal jacking stress.

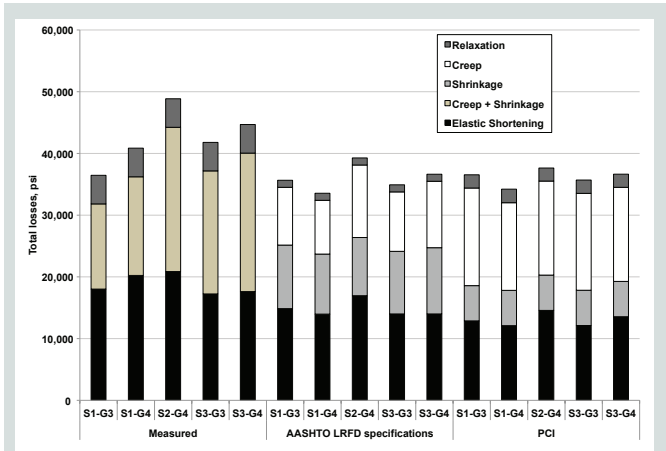


Figure 3. Comparison of total prestress losses. Note: 1 psi = 6.895 kPa.

of the SCC girders (both high-strength SCC and normal-strength SCC) averaged 45.1 ksi (311 MPa), or 22.6% of the nominal jacking stress. In general, elastic shortening losses represented 44.4 % of the total losses. However, time-dependent losses due to creep and shrinkage were less than the elastic shortening losses for measured values in all monitored girders.

Predicted total prestress loss values according to the AASHTO LRFD specifications and the *PCI Design Handbook* underestimated the measured total strain. Surprisingly, the AASHTO LRFD specifications and *PCI Design Handbook* methods showed good agreement with measured losses for HSC girders. Losses computed using the *PCI Design Handbook* method with measured parameters resulted in underpredictions of total prestress losses. However, the calculated losses using this method are closer in magnitude to the measured losses than the losses calculated using the AASHTO LRFD specifications method with measured parameters (**Fig. 3**). Based on this analysis, for precast, prestressed HSC, high-strength SCC, and normal-strength SCC, the *PCI Design Handbook* and AASHTO LRFD specifications methods are recommended for prestress loss estimation in the design stage. The average difference between the values calculated according to these methods and the measured values was less than 20%.

Figure 4 displays the total measured prestress losses for HSC, high-strength SCC, and normal-strength SCC. The high-strength SCC girders had high total prestress loss overall. However, the data are not normalized to take differences in girder length into account. The normalized values indicate that the total loss over a unit length is about 6% less for high-strength SCC than for normal-strength SCC. Furthermore, as could be anticipated, HSC showed total prestress losses of lower magnitude than those of high-strength SCC and normal-strength SCC.

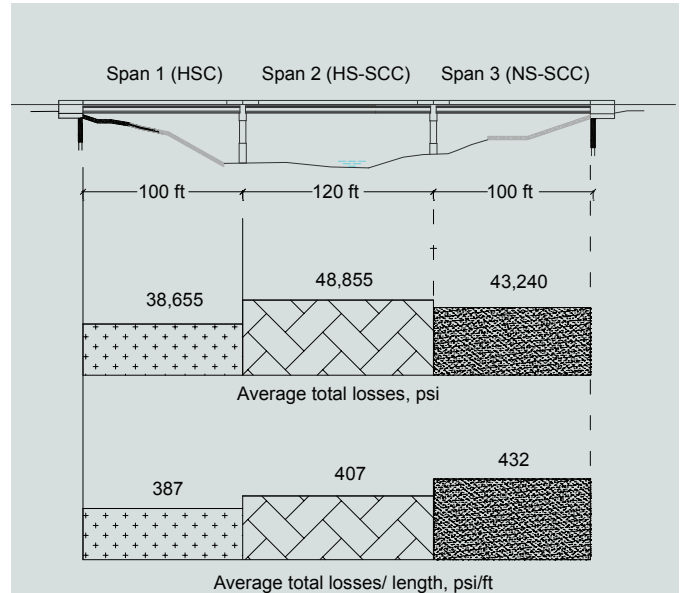


Figure 4. Average total prestress losses. Note: HS = high-strength; HSC = high-strength concrete; SCC = self-consolidating concrete. 1 ft = 0.305 m; 1 psi = 6.895 kPa.

Comparison with previously collected data

Experimental data of measured prestress losses reported in the literature were used to make a comparison with measured prestress losses of the bridge A7957 girders. The collected data^{7,21,23–28} contain results that were monitored to evaluate prestress loss in pretensioned beams or girders. The data set contains a total of 58 girder members and includes bridge members located throughout the United States in a variety of environmental conditions and with varying concrete mechanical properties, curing regimes, and geometries. To understand each case study presented in the literature, the cross-sectional area, length, compressive strength, and modulus of elasticity of each specimen were also collected and reported as associated with elastic shortening and total prestress loss. These details provide a clear idea regarding the total prestress losses in each case study. Various prestress loss measurement techniques were used on the specimens; however, a vibrating wire strain gauge was used for most of the collected data. The main objective of this effort was to compare the prestress losses of the bridge A7957 girders with the data reported in the literature and to check whether the total prestress losses of bridge A7957 fall within the collected data range and whether any trends appear.

The collected data were classified into three groups according to concrete type. The first group, with 17 pretensioned girders, was for HSC with a compressive strength greater than 8000 ksi (55 MPa). The second group comprised data for high-performance concrete, with 33 cases included. The remaining set of eight data points was

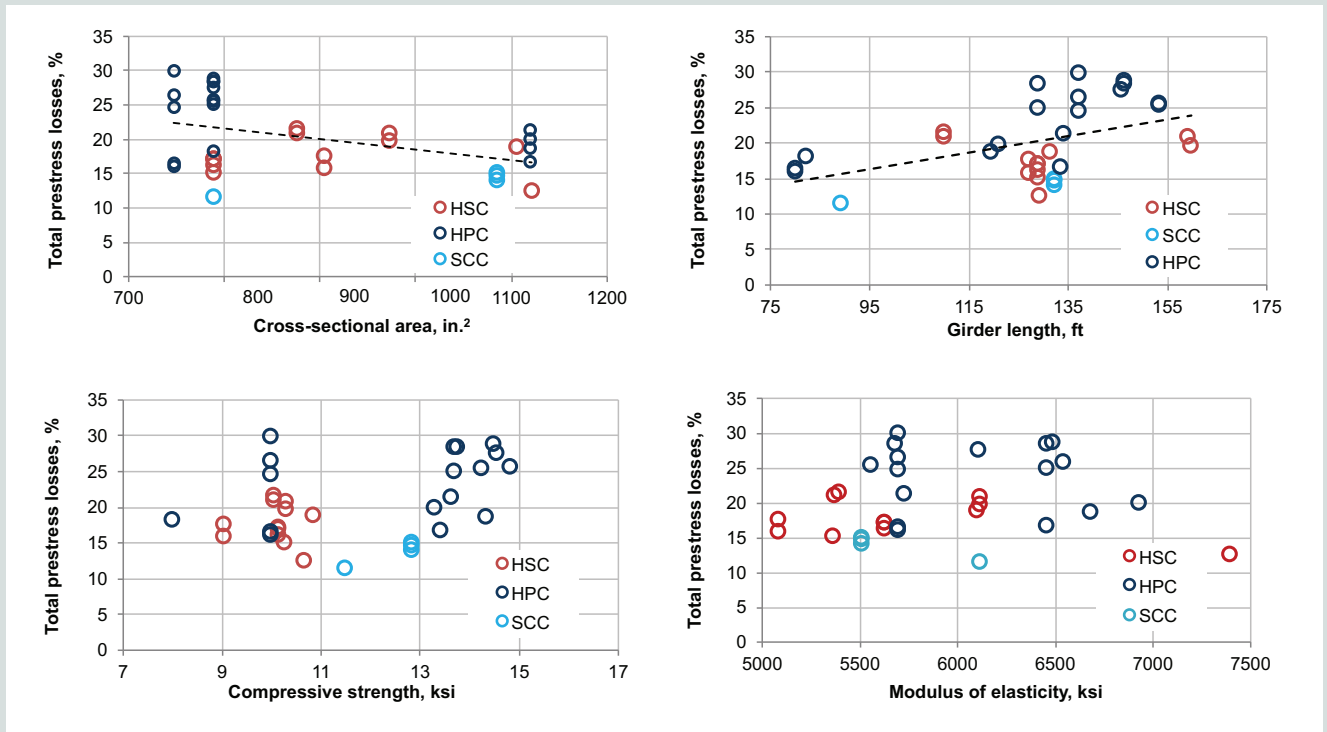


Figure 5. Total measured prestress losses as a percentage of the nominal jacking stress versus various parameters. Note: HPC = high-performance concrete; HSC = high-strength concrete; SCC = self-consolidating concrete. 1 ft = 0.305 m; 1 in.² = 645.2 mm²; 1 ksi = 6.895 MPa.

for SCC. For the specific data set, Alghazali and Myers²⁹ has the data in tabular format.

From the data set, the authors concluded that the total measured prestress losses, including elastic shortening, creep of concrete, shrinkage of concrete, and relaxation of the tendon for all girders ranged from 10% to 35 % of the nominal jacking stress. Because bridge A7957 losses were 19.2% and 22.6% for HSC and SCC, respectively, these results fall within the range of the compiled data. Furthermore, the HSC data exhibit less variance than other classes of concrete.

After the results were inspected, an effort was made to examine the effects of various parameters, such as specimen length, concrete compressive strength, modulus of elasticity, and geometry, on the total prestress loss. The data were filtered to extract all relevant information from each study and eliminate the results that were considered outliers. This resulted in 33 specimens to be analyzed for these effects. The total prestress losses decrease as the cross-sectional area increases, while increasing specimen length leads to an increase in the total prestress loss (Fig. 5). In addition to geometry effects, the mechanical properties (compressive strength and modulus of elasticity) did not show any general trend with total prestress loss (Fig. 5).

Conclusion

This full-scale study was conducted to determine the long-term behavior of prestressed HSC, high-strength SCC, and normal-strength SCC beams. Based on this research, the following conclusions can be drawn:

- A data acquisition system and vibrating wire strain gauges were successfully installed and are functioning adequately to collect strains and temperatures in the girders of bridge A7957 during fabrication, erection, and service life.
- The measured elastic shortening losses for HSC, high-strength SCC, and normal-strength SCC averaged 19.13, 20.87, and 17.43 ksi (131.9, 143.9, and 120.2 MPa), respectively. For all girders, the measured elastic shortening losses were higher than predicted using gross cross section and measured or predicted modulus of elasticity.
- The average ratios of measured to predicted elastic shortening according to the AASHTO LRFD specifications and the *PCI Design Handbook* were between 1.21 and 1.67 for HSC and between 1.35 and 1.43 for high-strength SCC. For normal-strength SCC, the

ratios of measured to predicted losses were between 1.23 and 1.42. The difference between the measured and predicted values might be due to resistance to the shortening of the girders before the release, which could cause losses to appear artificially high. It might also be explained by the differences between the actual modulus of elasticity and the values determined from companion specimen tests.

- For all girders, elastic shortening losses accounted for the largest component of the total measured loss.
- Both the AASHTO LRFD specifications and *PCI Design Handbook* empirical models underestimated the elastic shortening losses of HSC, high-strength SCC, and normal-strength SCC based on either the actual or predicted modulus of elasticity.
- The total prestress losses averaged 38.65, 48.85, and 43.24 ksi (266.5, 336.8, and 298.1 MPa) for the HSC, high-strength SCC, and normal-strength SCC girders, respectively.
- For most girders, the total measured prestress losses were greater than predicted using the AASHTO LRFD specifications and *PCI Design Handbook* methods.
- In general, the AASHTO LRFD specifications method tended to be more accurate than the *PCI Design Handbook* method in predicting HSC prestress losses.
- The total prestress losses in the compiled data included elastic shortening, creep of concrete, shrinkage of concrete, and relaxation of strand for all girders ranged from 10% to 35% of the nominal jacking stress. Because bridge A7957 losses were 19.2% and 22.6% for HSC and SCC, respectively, these results fall within the range of the compiled data. Furthermore, the HSC results data exhibit less variance than other types of concrete.

Acknowledgments

The authors gratefully acknowledge the financial support provided by the Missouri Department of Transportation and the National University Transportation Center at the Missouri University of Science and Technology (Missouri S&T). They also wish to thank the support received from both the department of Civil, Architectural and Environmental Engineering and the Center for Infrastructure Engineering Studies at Missouri S&T.

References

1. Myers, J. J., and K. E. Bloch. 2013. *Innovative Concrete Bridging Systems for Pedestrian Bridges: Implementation and Monitoring*. National University Transportation Center Report R250. Rolla, MO: Center for Transportation Infrastructure and Safety, Missouri University of Science and Technology.
2. ACI (American Concrete Institute) Committee 363. 2010. *Report on High-Strength Concrete*. ACI 363R-10. Farmington Hills, MI: ACI.
3. Daczko, J. A. 2012. *Self-Consolidating Concrete: Applying What We Know*. Abingdon, UK: Spon Press.
4. ACI Committee 237. 2007. *Self-Consolidating Concrete*. ACI 237R-07. Farmington Hills, MI: ACI.
5. Alghazali, H. H., and J. J. Myers. 2015. "Creep and Shrinkage of Ecological Self-Consolidating Concrete". In *Second International Conference on Performance-based and Life-cycle Structural Engineering (PLSE 2015) Proceedings, December 9–11, 2015, Brisbane, Australia*. St. Lucia, Australia: University of Queensland.
6. AASHTO (American Association of State Highway and Transportation Officials). 2012. *AASHTO LRFD Bridge Design Specifications*. 6th ed., customary U.S. units. Washington, DC: AASHTO.
7. PCI Industry Handbook Committee. 2010. *PCI Design Handbook: Precast and Prestressed Concrete*. MNL-120. 7th ed. Chicago, IL: PCI.
8. Roller, J. J., H. G. Russell, R. N. Bruce, and W. R. Alaywan. 2011. "Evaluation of Prestress Losses in High-Strength Concrete Bulb-Tee Girders for the Rigolets Pass Bridge." *PCI Journal* 56 (1): 110–134.
9. Brewe, J. E., and J. J. Myers. 2010. "High-Strength Self-consolidating Concrete Girders Subjected to Elevated Fiber Stresses, Part 1: Prestress Loss and Camber Behavior." *PCI Journal* 55 (4): 59–77.
10. ASTM Subcommittee A09.60.2010. *Standard Test Method for Air Content of Freshly Mixed Concrete by the Pressure Method*. ASTM C231/C231M-10. West Conshohocken, PA: ASTM International.
11. ASTM Subcommittee A09.47.2009. *Standard Test Method for Slump Flow of Self-Consolidating Concrete*. ASTM C1611/C1611M-09. West Conshohocken, PA: ASTM International.
12. ASTM Subcommittee A09.47.2008. *Standard Test Method for Passing Ability of Self-Consolidating Concrete by J-Ring*. ASTM C1621/C1621M-08. West Conshohocken, PA: ASTM International.

13. ASTM Subcommittee A09.47.2010. *Standard Test Method for Static Segregation of Self-Consolidating Concrete Using Column Technique*. ASTM C1610/C1610M-10. West Conshohocken, PA: ASTM International.
14. ASTM Subcommittee A09.60.2012. *Standard Test Method for Temperature of Freshly Mixed Hydraulic-Cement Concrete*. ASTM C1064/C1064M-12. West Conshohocken, PA: ASTM International.
15. ASTM Subcommittee A09.61.2012. *Standard Test Method for Compressive Strength of Cylindrical Concrete Specimens*. ASTM C39/C39M-12a. West Conshohocken, PA: ASTM International.
16. ASTM Subcommittee A09.61.2010. *Standard Test Method for Static Modulus of Elasticity and Poisson's Ratio of Concrete in Compression*. ASTM C469/C469M-10. West Conshohocken, PA: ASTM International.
17. ASTM Subcommittee A09.61.2010. *Standard Test Method for Flexural Strength of Concrete (Using Simple Beam with Third-Point Loading)*. ASTM C78/C78M-10. West Conshohocken, PA: ASTM International.
18. ASTM Subcommittee A01.95.2011. *Standard Practice for Use of Apparatus for the Determination of Length Change of Hardened Cement Paste, Mortar, and Concrete*. ASTM C490/C490M-11. West Conshohocken, PA: ASTM International.
19. ACI Committee 318. 2014. *Building Code Requirements for Structural Concrete (ACI 318-14) and Commentary (ACI 318R-14)*. Farmington Hills, MI: ACI.
20. Alghazali H. H., and J. J. Myers. 2015. "High Strength Self Consolidating Concrete Prestress Losses of Bridge A7957, MO, USA Compared to Code Models." In *Fifth International Conference on Construction Materials: Performance, Innovations and Structural Implications (ConMat'15) Proceedings, August 19–21, 2015, Whistler, BC, Canada*. Vancouver, BC, Canada: University of British Columbia.
21. Gross, S. P. 1999. "Field Performance of Prestressed High Performance Concrete Highway Bridges in Texas." PhD diss., University of Texas at Austin.
22. Nawy, E. G. 2009. *Prestressed Concrete: A Fundamental Approach*. 5th ed. Upper Saddle River, NJ: Prentice Hall.
23. Tadros, M. K., N. Al-Omaishi, S. J. Seguirant, and J. G. Gallt. 2003. *Prestress Losses in Pretensioned High-Strength Concrete Bridge Girders*. NCHRP (National Cooperative Highway Research Program) report 496. Washington, DC: Transportation Research Program.
24. Trejo, D., M. B. Hueste, Y. Kim, and H. Atahan. 2008. *Characterization of Self-consolidating Concrete for Design of Precast Prestressed Bridge Girders*. Report 0-5134-2. College Station, TX: Texas Transportation Institute.
25. Ruiz, E. D., R. W. Floyd, B. W. Staton, N. H. Do, and W. M. Hale. 2008. *Prestress Losses in Prestressed Bridge Girders Cast with Self-consolidating Concrete, MBTC-2071*. Fayetteville, AR: Mack-Blackwell Rural Transportation Center, University of Arkansas.
26. Myers, J. J., and Y. Yang. 2005. *High Performance Concrete for Bridge A6130-Route 412 Pemiscot County, Missouri*. UTC R39. Rolla, MO: University of Missouri–Rolla.
27. Barr, P., M. Eberhard, J. Stanton, B. Khaleghi, and J. C. Hsieh. 2000. *High Performance Concrete in Washington State SR18/SR516 Overcrossing: Final Report on Girder Monitoring*. Seattle, WA: Washington State Transportation Center (TRAC).
28. Waldron, G. J. 2004. "Investigation of Long-Term Prestress Losses in Pretensioned High Performance Concrete Girders." PhD diss., Virginia Polytechnic Institute and State University.
29. Alghazali, H. H., and J. J. Myers. 2016. "A Study of Elastic Shortening Losses of High-Strength Self-Consolidating Concrete Prestress Girders." *International Journal of Research in Engineering and Science* 4 (9): 6–16.

Notation

A	= cross-sectional area
A_g	= gross section area
e	= eccentricity of the strand
E_c	= concrete modulus of elasticity
E_{ci}	= modulus of elasticity of the concrete at release
E_{ps}	= modulus of elasticity of the prestressing strands

f'_c	= concrete compressive strength	M	= moment applied to the beam
f_{cgs}	= concrete stresses at the center of gravity of the prestressing steel due to prestressing force at release and self-weight of member at sections of maximum moment	p	= predicted loss
f'_{pi}	= initial stress of prestressing tendons	P	= estimated force immediately after release
f_{py}	= specified yield strength of prestressing tendons	t	= time after prestressing
I_g	= gross moment of inertia (uncracked section)	w_c	= concrete density
L	= length of beam or girder	$\Delta f_{ES, Calculated}$	= calculated change in stress from elastic shortening
m	= measured loss	$\Delta f_{ES, Measured}$	= measured change in stress from elastic shortening
		ϵ_{cgs}	= strain at the centroid of the prestressing steel

About the authors



Hayder Alghazali is a PhD candidate in the Civil, Architectural and Environmental Engineering Department at Missouri University of Science and Technology in Rolla, Mo.



John J. Myers, PhD, PE, FACI, FASCE, FTMS, is a professor in the Civil, Architectural and Environmental Engineering Department, director of the Structural Engineering Research Laboratory, and associate vice provost and dean in the College of Engineering and Computing at Missouri University of Science and Technology.

Abstract

In this study, six precast, prestressed concrete girders were constructed and instrumented to measure prestress losses of bridge A7957 in Missouri. The concrete mixture for the bridge was designed with varying mechanical and rheological properties. High-strength concrete, high-strength self-consolidating concrete,

and normal-strength self-consolidating concrete were used to construct the bridge girders. Vibrating wire strain gauges with integrated thermistors were embedded through the girders' cross sections to measure strains and temperatures. The measured short- and long-term prestress losses were compared with those obtained using different empirical models, specified in the *AASHTO LRFD Bridge Design Specifications* and in the *PCI Design Handbook: Precast and Prestressed Concrete*. This study also presents a comparison of measured prestress losses with data reported in the literature for different concrete types.

Keywords

Bridge, girder, high-strength concrete, high-strength concrete, normal-strength concrete, prestressed, prestress loss, self-consolidating concrete, strain.

Review policy

This paper was reviewed in accordance with the Precast/Prestressed Concrete Institute's peer-review process.

Reader comments

Please address reader comments to journal@pci.org or Precast/Prestressed Concrete Institute, c/o *PCI Journal*, 200 W. Adams St., Suite 2100, Chicago, IL 60606. **■**